Detecting Critical Slowing Down by Estimating the Recovery Period after Fire Using NDVI Time Series in a Mediterranean-climate Forest Ecosystem

Fatemeh Mahmoudi
February, 2014

Detecting Critical Slowing Down by Estimating the Recovery Period after Fire Using NDVI Time Series in a Mediterranean-climate Forest Ecosystem

by

Fatemeh Mahmoudi

Thesis submitted to the Faculty of Geo-Information Science and Earth Observation of the University of Twente in partial fulfilment of the requirements for the degree of Master of Science in Geo-information Science and Earth Observation, Specialisation: (GEM)

SUPERVISORS:

Dr. T.A. (Thomas) Groen
Dr. A. (Anton) Vrieling

Advisor:
Dr. N.C. (Niels) Brouwers
(Murdoch University, Australia)

Thesis Assessment Board

Name Examiner 1 (Chair): Dr. A.G. (Bert) Toxopeus
Name Examiner 2: Dr. ir. Frank van Langevelde (Wageningen University)


ITC
UNIVERSITY OF TWENTE.
FACULTY OF GEO-INFORMATION SCIENCE AND EARTH OBSERVATION

Disclaimer

This document describes work undertaken as part of a programme of study at the Faculty of Geo-Information Science and Earth Observation of the University of Twenty. All views and opinions expressed therein remain the sole responsibility of the author, and do not necessarily represent those of the institute.

Abstract

In this paper, the effect of fire frequency and drought on forest recovery period after fire disturbance was analysed by means of remote sensing imagery and a fire history dataset in Northern Jarrah Forest (NJF). Fourteen years of 10-daily SPOT NDVI images from mid-1998 to mid-2013 were employed to detect fire signals, to estimate the forest recovery period and to assess the relationship between recovery period and both fire frequency and relative drought. Fire signals were detected by comparing the NDVI temporal profile of a pixel to unburned neighbouring control sites. The spatial fire history dataset were used for site selection and to compare the NDVI-derived fire signals to the recorded fires. The ratio between the NDVI values with the NDVI of its neighbours is referred here as the forest state index (RE). Significant declines in RE were interpreted as a signal of fire. Moreover, the RE value served to evaluate post-fire recovery times. Results show different patterns of recovery for each selected burned site based on time of occurrence. The user's accuracy of this prediction was about 41%, which is relatively good given the uncertainty in the input data. For all cases, a non-significant correlation was found between recovery period and fire frequency. This suggests, recovery period was not affected by the fire frequency in NJF. It can be concluded that this system may be adapted to the fire. Also the results showed a longer recovery period for burned sites with high amount of precipitation in the month of fire and during the recovery period. Critical slowing down may not happen in this system as a result of fire frequency, but high uncertainty in the results may also account for the absence of evidence in this regard.

Acknowledgements

First and foremost I would like to thank God. You have given me the power to believe in myself and pursue my dreams. I could never have done this without the faith I have in you.

I would like to express my very great appreciation and thanks to my supervisors, Dr. Thomas Groen and Dr. Anton Vrieling for their willingness to give their time so generously, valuable and constructive advice, recommendations and helpful ideas to improve my work in all the time of research and writing of this thesis. I would like to thank you for encouraging my research and for allowing me to grow as a research scientist.

I would also like to thank Dr. Niels Brouwers for his support and providing relevant datasets at the beginning of my project. I would like to thank Mr. Willem Nieuwenhuis (software developer in ITC, University of Twente) for providing several programing scripts for my meteorological data.

I take this opportunity to express a deep sense of gratitude to all of my teachers and staff here in ITC Faculty of Geoinformation and Earth Observation Science and in the Department of Physical Geography and Ecosystem Modelling at Lund University for their assistance, kind hospitality and endless support during my studies.

I would like to thank all of my friends and colleagues at both ITC and Department of Physical Geography and Ecosystem Modelling at Lund University. I would also like to express appreciation to all of my friends who supported me in writing, and incanted me to strive towards my goal.

I am also very grateful to Erasmus Mundus for its financial support for this programme.

At the end a special thanks to my family. Words cannot express how grateful I am to my mother and father, who have always given me the strength and wisdom to be sincere in my work, for setting high moral standards and supporting me through their hard work, and for their unselfish love and affection. Your prayer for me was what sustained me thus far. This dissertation is dedicated to them.

Table of Contents

List of figures

List of tables

1. Introduction

1.1 Background information

Forest collapse and degradation is one of the ecologists concerns, because forests play an important role in human's economic and social life. Forests secure environmental functions such as providing clean water, sequestering carbon and controlling erosion, and play an essential role in providing habitats for fauna and flora. According to FAO (2006), forests are major reservoirs of terrestrial biodiversity and include over 50% of the global terrestrial biomass carbon stocks. However, continued degradation and deforestation has contributed to increasing concentrations of CO_2 and other greenhouse gases into the atmosphere (Beerling, 1993). The increased emissions of greenhouse gases have resulted in recent increases of global mean temperature (about 0.5 °C since 1970) (IPCC, 2007). Climatic incidents ranging from ice storms to typhoons can destruct forests, but it has been identified that forest mortality has increased due to climate-induced stress such as drought and raised temperatures around the globe (Allen et al., 2010). Understanding and forecasting the effects of these climatic changes on ecosystems is an ongoing challenge for scientists.

Different ecosystems respond differently to gradually changing environmental conditions. Climate, groundwater reduction and loss of species diversity are some examples of conditions within ecosystems, which change gradually and smoothly with time (Tilman et al., 2001). Besides smooth changes (Figure 1-1. a), the response of ecosystems to changing conditions (e.g. drought) may be quite intense when conditions reach a critical point (Figure 1-1. b). Sometimes, an ecosystem may respond completely differently to changing conditions when its equilibrium state bends backwards under the assumption that such an ecosystem has two alternative stable states for the same environmental conditions (i.e. drought here) (Figure 1-1. c). When the state of an ecosystem is on the upper equilibrium, it cannot switch to the lower equilibrium smoothly but when there is a sufficient change in conditions, a 'catastrophic' shift to the lower branch takes place after passing a threshold (F2) which is often referred to as the tipping point (Scheffer et al., 2001).

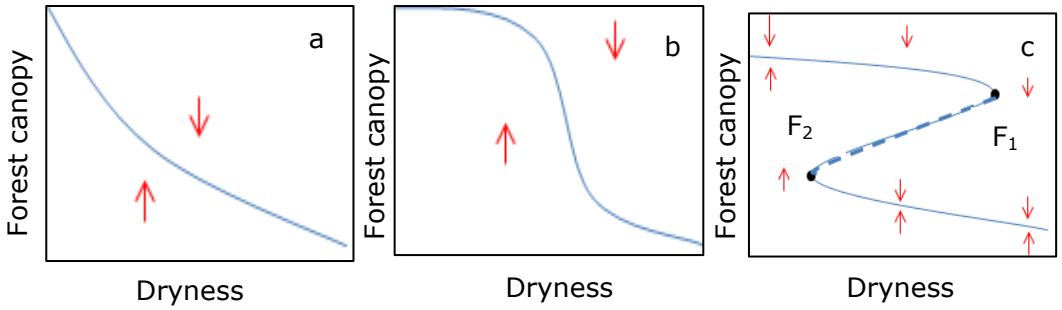

Figure 1-1. This figure illustrates the possible responses of ecosystem equilibrium states which can vary due to conditions. In (a) and (b) there is only one equilibrium for each condition but in (c) the equilibrium curve bended backward and in given condition three equilibria exist. The dashed equilibrium is unstable and displays the border between two alternative stables.

Sudden shifts in ecosystem states, caused by changing environmental conditions, have been shown in different ecosystems (Scheffer et al., 2001). Shifts from one state to another alternative stable state can occur in lakes also (Carpenter et al., 1999). One example of drastic shift in this ecosystem is an abrupt loss of water clarity and vegetation in shallow lakes due to nutrient concentrations (Scheffer et al., 1993). Remarkably, water transparency can be hardly affected by nutrient loading, unless it passes a critical transition, at which a sudden shift from clear to turbid state occurs. This increased turbidity causes the loss of vegetation and consequently loss of algal biomass and animal diversity which makes this state undesired. Shifts from savannahs (sparse tree with grass layer) to a dense woody state as an alternative stable state is another example which can occur due to a combination of fire and grazing regimes change (Ludwig et al., 1997). Extreme grazing decreases the grass and also fuel for fire while natural fires decrease the woody plant cover and increase the grass layer. In the fire absence, shrubs growth starts during the wet period and can overwhelm the grass cover, so fire spread is prevented. The system stays in this state until trees begin to die and allow the grass layer to make fuel for an effective fire. These processes of shifting from one state to another contrasting state are known as 'critical transitions', where critical means that the shift is irreversible or costly to reverse (Folke et al., 2004). As explained before, critical transitions can occur when the system approaches a tipping point (Dakos et al., 2008). Although critical transitions cannot be easily predicted, especially for complex systems, certain generic signals known as "early warning signals" may occur in the ecosystems when approaching a tipping point.

An important early warning signal is a phenomenon known as 'critical slowing down' (Van Nes and Scheffer, 2007, Wissel, 1984). When a system approaches a tipping point, it needs increasingly more time to recover from regular common disturbances. There are some statistics that can indicate the 'critical slowing down' process such as an increase in variance, skewedness, and autocorrelation of the rate of recovery of a repeatedly disturbed system compared to an undisturbed stable system (Dakos et al., 2012). According to Scheffer et al. (2001), resilience lost in a system makes it easier for a system to switch to an alternative state. Following Van Nes and Scheffer (2007), in this study, resilience is considered as the ability of the system to return to the equilibrium that existed before perturbation. A reduction of a system's resilience can thus be inferred from a declining ability to recover, for example, for Mediterranean ecosystems after increased fire disturbance by Diaz-Delgado et al. (2002). The use of recovery rates after a disturbance as a general indicator provides a chance to study the resilience of forest ecosystems and possibly predict the approach of a catastrophic shift (Scheffer et al., 2009).

Time series of remotely-sensed data could provide a useful input to monitor disturbances and recovery rates in ecosystems. For regional and global monitoring of terrestrial ecosystems, regular and consistent records of remote sensing images offer spatial information on the temporal dynamics (Tarnavsky et al., 2008). An example of remotely-sensed data is the frequent (daily) information on green vegetation cover offered by coarse-resolution optical satellite sensors such as AVHRR (Advanced Very High Resolution Radiometer), SPOT (Système Pour l'Observation de la Terre) VEGETATION, and MODIS (Moderate Resolution Imaging Spectroradiometer). A common index that can be extracted from these sensors is the Normalized Difference Vegetation Index (NDVI), which combines information from reflection measured by a sensor in red and near infrared (NIR) wavelength bands. It uses the high absorbance of radiation by healthy green vegetation in the red band and the high reflectance of vegetation in the NIR band of the electromagnetic spectrum and is computed from reflectance images (Equation 1).

$$NDVI = (\rho NIR - \rho RED)/(\rho NIR + \rho RED) \qquad \text{Equation (1)}$$

The NDVI relates to the amount of green biomass, and has been used as a proxy indicator for the total amount of biomass (Anderson et al., 1993), and vegetation density and health (Lotsch et al., 2003). When evaluating NDVI over time, information on how greenness changes was obtained within a year, and between years. For forest

ecosystems, for example, NDVI time series may help to identify disturbances, and to assess the recovery to normal conditions of the ecosystem.

Catastrophic forest loss caused by extreme weather conditions such as drought and heat is increasingly being reported (Granzow-de la Cerda et al., 2012). A good example is the abrupt and unprecedented forest collapse in Mediterranean-type forest (MTF) in western Australia, which likely relates to drought and heat conditions in 2010/2011, despite the fact that forests here are considered to be drought-resilient (Matusick et al., 2013). This event brings concern that more abrupt and catastrophic forest collapses may occur in the future, and illustrates the necessity for aiming at better predicting, and hopefully preventing, future forest collapses. One possible avenue towards improved prediction is to follow the critical slowing down theory, and assess how recovery currently takes place after perturbations to the system.

Most studies that examined the critical slowing down theory were model-based, while only a few studies found signals of slowing down in real ecosystems with natural perturbations (Dakos et al., 2010, Scheffer et al., 2009). This study is an attempt to contribute real evidence for the theory using a case study of the Australian Jarrah forest system that is regularly disturbed due to natural fires. In this research, spatial and temporal variability in the recovery period after fires for the Northern Jarrah Forest system in the Southwest Australian Floristic Region (SWAFR) was studied. This region was suitable for this research project because it is increasingly being affected by a drying and warming climate (CSIRO and BOM, 2007), and because forest collapses have been observed as a result of drought and heat condition (Matusick et al., 2013)

To gain a better understanding of the fire impacts on forests, it is important to know how fire affects the forest vegetation. The effect of fire on plant communities depends on the species present (e.g., resprouter vs. non-resprouting species) and their life cycle stage (i.e., maturity level, carrying seed or not). Long-term effects of fire on plants are considered within fire regime components which are fire intensity, fire frequency and season of fire occurrence (Gill, 1975). Fire impact on vegetation differs based on its intensity level. A 'low intensity fire' burns understorey and scorches overstorey trees, trunk and crown while a 'high intensity fire' burns understorey and overstorey. Fires occurring in the spring with low intensity disturb grass-shrub understory and go out at night due to increased relative humidity and cooler air. Early dry season fires occur when fuel

moisture is high from winter rainfall. This moist in the fuels has an effect on fire behaviour which results in less intense fires with low speed and flame height (Government Of Western Australia, 2013). In contrast, in summer (late in the dry season), fuels get drier because of sun and wind, the fires get more flammable, and fire intensity increases. These fires eliminate grassy fuels and continue overnight (Government Of Western Australia, 2013). If fuels are extensive, mostly overstory trees are damaged (Goldammer, 1990). Similar to spring, autumn fires occur with increased moisture in the dry summer fuels due to opening seasonal rains. Fire intensity and behaviour is modified by moist fuels and cool weather after the first rains in autumn. However in comparison to spring, the landscape is much drier, thereby, uniform burn of canopies is more common in autumn. According to Gill (1975), in the forests of southwest and southeast Australia, fires are less frequent but more severe.

The overall effect of fire on the different forest components depends on fire type as well. Ground fires only have a strong impact on soil, which has organic matter and can have a very negative consequence for trees due to their damage on root systems. However, surface fires burn grass, dead plant and twig material lying on the ground and scorch tree trunks and crowns. Crown fires mostly affect tops of shrubs and trees. Ecosystems may experience one or a mixture of these fire types (Bond and Keeley, 2005).

In tropical forests, except from burning by humans, there can be a climatic explanation for more fires as result of, for example, increased drought, increased evapotranspiration, and decreased summer rainfall. Increased evapotranspiration and decreased summer rainfall will cause more severe and longer-lasting droughts. Through prolonged and frequent droughts, vegetation loses its moisture and becomes more flammable, consequently drought frequency has the potential to raise the probability of wildfires (UOC, 2003). Rainfall during the growing season increases the vegetation moisture and decreases their flammability. This moisture in the vegetation reduces the fire intensity and speeds the recovery process. High amount of rainfall during the fire event cools down the fire and causes highly wet vegetation and less intense fire with a little damage to forest which takes shorter for the forest to recover. A lot of rain after fire (during the recovery period) would shorten the recovery period due to a lot of water availability, which helps the vegetation to green-up quickly. As mentioned before, the recovery and green-up after fire is highly dependent on the season the fire took place. Summer burns (Dec-Feb) are more intense and often wildfires. With a little water availability, the vegetation will take much longer to green-up again to

the original level (6-12 months). For spring fires, (September - November) green-up occurs gradually over a period of 2-3 months.

1.2 Research objectives

The aim of this research is to assess whether forest fire signals and post-fire recovery time can be accurately determined with NDVI time series for selected locations of the Northern Jarrah Forest (NJF) in order to evaluate if critical slowing down is occurring in this ecosystem. Our assumption is that NDVI is a good indicator to detect fire signals in the NJF, which can then be verified by the fire history dataset. Based on this hypothesis the following objectives were formulated:

1. To evaluate if NDVI time series can unambiguously detect fire signals in the study area.
2. To estimate the time that a fire-affected forest area needs to recover to the normal seasonal NDVI cycle.
3. To test whether the recovery period increases for higher levels of drought and fire frequency.

1.3 Research questions

1. Can the fire signals be detect in the study area using NDVI time series based on the fire occurrence in a specific period?
2. Is it possible to observe forest recovery after fire from NDVI time series and estimate time to recover to normal seasonal cycle?
3. Is forest recovery period increasing when fire frequency is increasing?
4. Is forest recovery period increasing when drought is increasing?

1.4 Research hypothesis

1. Hypothesis 1: Main fire events in the observational fire dataset will cause a significant decline in NDVI values for locations where this fire occurred.
2. Hypothesis 2: After a clear drop in NDVI, it is increased to normal state which will represent the recovery period.
3. Hypothesis 3: An increase in fire frequency will increase the recovery time of forest after fire.
4. Hypothesis 4: Dry conditions (before, during and/or after) will increase the recovery time of forest after fire.

2. Description and background of dataset

2.1 Description of dataset

For this research, SPOT VEGETATION 10-daily Normalized Difference Vegetation Index (NDVI) images, from mid-1998 to mid-2013 were used. These images are freely available through http://www.vito-eodata.be/PDF/portal/Application.html#Home. Although other vegetation metrics can be used, NDVI was selected due to its availability at a good spatial (1 km by 1 km) and temporal (every 10 days) resolution compared to the extents and timing of burned areas. This data set is constructed based on daily radiance information recorded by the VEGETATION sensor on-board the SPOT 4 platform (launched in March 1998), and the SPOT 5 platform (launched in May 2002). Based on the daily observations, 10-daily temporal NDVI composites are produced using the maximum-value compositing technique to reduce atmospheric effects in the series. For each pixel, the daily recording with the highest NDVI (and a close-to-nadir view angle) is retained in the dataset. This product is referred to as S10 and is available in three different spatial resolutions: 1, 4 and 8 km. In this study, the 1-km resolution dataset was used. This data is in 8-bit unsigned binary format and can be converted to valid NDVI values with the following equation:

NDVI = (RAW*0.004) - 0.1 Equation (2)

The second dataset with the name of (AWAP\Run26h), which was used for assessing the effect of climate condition (drought), is monthly historical meteorological data at 5x5km resolution. This dataset includes precipitation (m/day), maximum temperature (°C) and minimum temperature (°C), and is freely available through the Australian Water Availability Project (AWAP) (www.eoc.csiro.au/awap/). Rainfall data are available from 1900 to 2012 and temperature from 1911 up to 2012. The dataset is provided by the Australian Bureau of Meteorology (BoM) and is generated by spatial interpolation of the BoM's network of rain gauges and weather stations. This product is generated by rescaling daily rainfall at the end of each month so that the sum of daily rainfalls matches the subsequent monthly reanalysis. From this dataset, meteorological data from 1998 to 2012 were used to match the available NDVI dataset.

The third dataset used for this study was an accurate digital fire history dataset in a shapfile format, which is generated on an annual

basis by the Department of Parks and Wildlife (DPaW), Western Australia, and includes data on the timing and extent of the fires that have occurred. This dataset contains a collection of records of fire events (prescribed burns and wildfires) of which the earliest records date back to 1937. Since NDVI images are available from 1998 in this study the focus was more on fires occurring after 1997. A world imagery group layer provided by ArcGIS online service was used for better investigation of site selection. This group layers present satellite imagery and aerial imagery for the world (http://goto.arcgisonline.com/maps/World_Imagery).

2.2 Background of dataset

The Jarrah Forest system is situated in the Southwest Australian Floristic Region (SWAFR). The Jarrah Forest is split into two regions, the Northern Jarrah Forest and the Southern Jarrah Forest. The study area for this research is the Northern Jarrah Forest (between Latitude 30°45´-33°30´S and Longitude 115°52´-117°5´E; Figure 2-1). The SWAFR region occupies 302,627 km^2, on a relatively wet continental region, surrounded on two sides by ocean, and isolated by arid lands to the north, northeast, and east (Hopper and Gioia, 2004). This region is one of the 34 global biodiversity hotspots, i.e., a region that is rich in endemic species and under threat due to anthropogenic and environmental pressures (Myers et al., 2000). This region contains nutrient-deficient landscapes which is rich in species, with 7,380 native vascular plants of which 2,500 are of conservation concern (Hopper and Gioia, 2004). The SWAFR is recognized as one of 10 Australian ecosystems that is highly vulnerable to climate shifts (temperature and rainfall), with the most sensitive habitats considered to be the dry sclerophyll (e.g. Jarrah) forests, woodlands and heathlands (Laurance et al., 2011). As in many parts of Australia, regular burning and wildfires occur in the SWAFR.

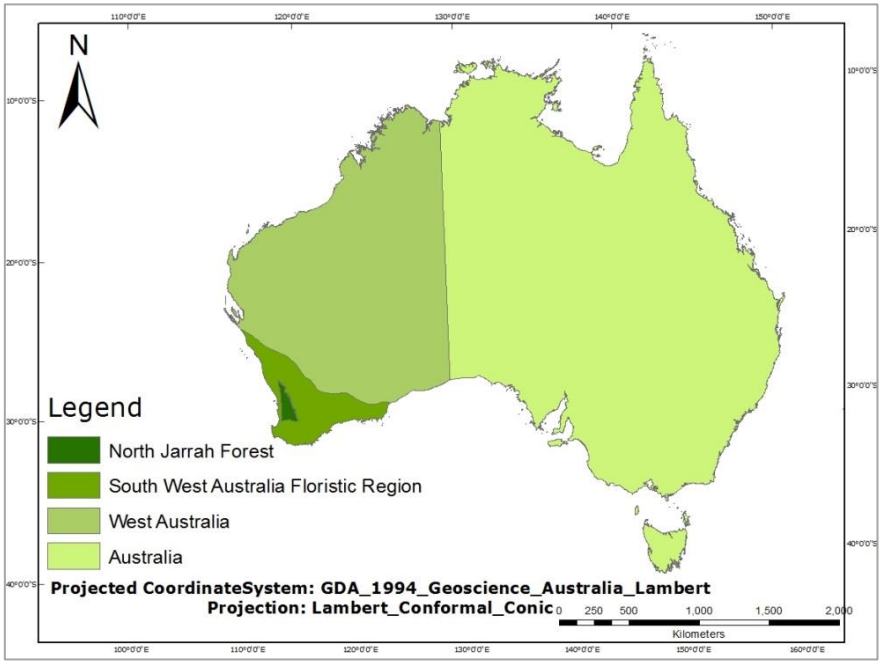

Figure 2-1. Study area in the Northern Jarrah Forest in southwest Australia

2.2.1 Climate

This region is among the Mediterranean climate regions, with warm to hot dry summers and mild to cool wet winters (Peel et al., 2007). The majority of rain falls from April to October (Bates et al., 2008) and dry season occurrence is from October to April, continuing for 2 to 7 months (Gentilli, 1989). Rainfall amount ranges between ~1,100 mm in the west to ~700mm in the east and north (Gentilli, 1989). Annual mean temperatures of this region have risen at a rate of +0.15°C per decade, and mean annual rainfall was approximately 14% lower in 1975-2004 as compared to pre-1975, with the main reduction in the May to July rainfall (Bates et al., 2008) (Figure 2-2). The majority of recent climate change models agree on the persistence of this trend, projecting a decrease in rainfall of up to 40% and an increase in temperature of up to 5 °C by 2070 (CSIRO and BOM, 2007). Mediterranean ecosystems is extremely sensitive to climate driven shifts (Klausmeyer and Shaw, 2009). SWWA is one of the regions, most likely to be affected, making it a priority for biodiversity conservations. Given the recent large-scale forest collapse in Mediterranean-type forest (MTF) in western Australia corresponding with dry and heat conditions in 2010/2011 (Matusick et al., 2013), it can be expected that these climatic shifts will result in more forest collapses. This strongly suggests that the resilience of these forest systems is increasingly being affected by the changes in climate,

which makes this study area a suitable site to evaluate the phenomenon of critical slowing down of forest recovery after disturbance.

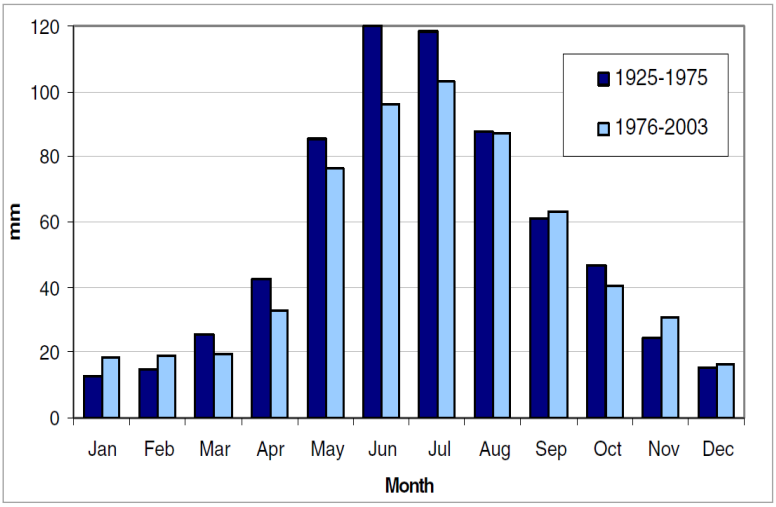

Figure 2-2. Average monthly rainfall (mm) for the southwest corner of Australia (Bates et al., 2008)

2.2.2 Vegetation species

The Northern Jarrah Forest (NJF) is an evergreen dry-sclerophyll broad-leaved forest, dominated by *Eucalyptus marginata* (jarrah) and commonly found with other *Eucalyptus* spp. species including *Eucalyptus wandoo* (wandoo), *Eucalyptus patens* (blackbutt) *and Corymbia calophylla* (marri). *Banksia grandis, Allocasuarina fraserani Persoonia* spp*, and Halkea* spp. are components of mixed midstory of this region (Heddle et al., 1980).

2.2.3 Forest structure

This forest is among those open forests in north and tall forest in south, in terms of canopy density. Moving from west to east and from south to north, as the rainfall decreases, forest decreases in density to woodland or low forests. Jarrah forms trees with 30-40 meter height and 2 meter diameter. This forest is among slow growing forest, averaging 1-2 cm increments in diameter decade. Large trees may be about 300 to 400 years old (Dell and Havel, 1989).

2.2.4 Fire adaptation

Jarrah forest has leached soils and accordingly has one of the most nutrient impoverished forest soils in the world (Dell and Havel, 1989).

In NJF the dominant species (i.e. *Eucalyptus marginata*) are very adapted to soil and climatic conditions. These species are adapted to fire with their capacity to resprout after fire from the seedling stage to maturity. They use their extensive root system to utilize the water from deep layer during the drought period, so other species barely can compete with them within the rainfall range 600–1300 mm on deep infertile soils (Dell and Havel, 1989).

3. Methods

In this research, sites with differences in fire history, and potentially in the recovery period, were compared. The identification of suitable sites was an important prerequisite for the subsequent steps of the analysis. Sites were grouped into two different classes:

1. Undisturbed sites (reference): Areas with no fire occurrence from mid-1997 to mid- 2013 were selected as reference sites. This was done by selecting the areas which did not exist in the fire history map.

2. Disturbed sites: Areas with one or more fire occurrences were selected using the steps explained in section 3.2.

3.1 Data preparation

SPOT VEGETATION 10-daily Normalized Difference Vegetation Index files were unzipped and stacked. Data for the ten day period covering 21 to 31 July 1999 were missing in the dataset and were filled up by interpolating between the previous and subsequent time steps. Similarly, the climatic data was unzipped and stacked for monthly 5x5km resolution images.

3.2 Site selection

For site selection, vector points were obtained from Raster NDVI by raster conversion. From the fire history dataset, areas which experienced the fire from 1997 onwards were subset, in order to have the history of fires corresponding to NDVI values. Following (Diaz-Delgado et al., 2002), calculation of the forest state index (RE) was needed for each site (both burned and unburned sites, Equation 3).

$$RE = \frac{b}{ub} \qquad \text{Equation (3)}$$

where b is NDVI of burned sites and ub is NDVI of unburned sites.

For this purpose, each RE is estimated by dividing of the NDVI values of two pixels, burned and unburned pixel which is as close as possible to the former. This was termed as pairwise selection. By the use of fire history map and imagery layer, unburned sites with their unburned neighbouring pixel (as reference pairs) and also burned and their nearby unburned sites were selected. It is worth to mention that among the characteristics of the pair, the date in which the fire occurred is known. In the next step, the following variables were

determined for each pair: fire frequency, time since last fire, and distance between the two pairs. These variables were filled in the attribute table while selecting the pairwise burned and adjacent unburned sites. In some cases, it was difficult or impossible to find areas which had not experienced fire as unburned sites. According to Dr. Niels Brouwers (personal communication, September 10, 2013) NDVI values recover in general 2-3 years after a Jarrah forest had burned, therefore areas which did not burn for 10 years or more were selected as an 'unburned' neighbouring sites. In some cases, even unburned sites with a fire history of 10 years since last fire could not be found, so only areas with a 'time since last fire age' of more than 5 years were considered in this site selection. All over, 30 pairs of unburned and 47 of burned sites were selected (Figure 3-1).

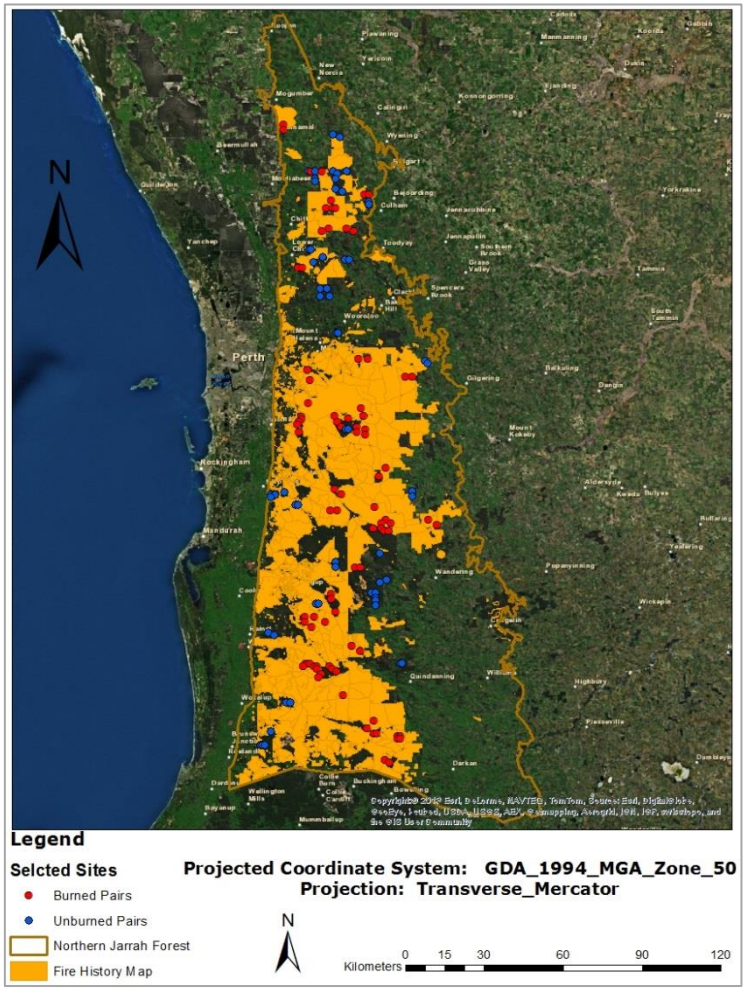

Figure 3-1. Selected burned and unburned sites in the Northern Jarrah Forest

3.3 Extracting time series

After site selection, NDVI values were assigned for all the defined locations. Having opened the file, some gaps or zero values were recognized. Zero indicates a land pixel with no NDVI by cause of quality control flagging (i.e. cloud/snow/ice). These zero values were filled out by interpolation in time (taking the average value of before and after). This approach was done because the NDVI values for missed pixels didn't show a significant difference in a temporal time of 10 days. Also missed data belong only to 1999/7/21 which, as mentioned before, was filled up by interpolating between the previous and subsequent time step as well. Then, the whole table was sorted out in a way that the burned pixel of pairwise sites was located in the upper row for calculating the ratio of each pair (burned/unburned). There were some noises in the data when it was plotted, and some outliers, which were consist only for a scene and appeared as "spikes or drops". These spikes and drops occur due to atmospheric problems. In order to keep the original data as much as possible, these outliers were kept in the data because it was expected these short fluctuations would not influence long term time series.

3.4 Effect of distance between pairwise sites on RE values

It was difficult and sometimes impossible to find a neighbouring unburned pixel for burned sites, so some unburned pixels were selected from longer distances. To assess whether their RE values are influenced by the effect of distance between them, neighbouring pixels were selected from different distances for reference sites. To examine the effect of distance between pairwise points on RE values, min, max, median, first quartile and third quartile of RE values for the whole period of the reference sites were calculated. Regression analysis was applied for median, first, and third quartile of RE values of 30 reference sites over distance to see the impact of distance on these values. Additionally, to be more precise in the estimation, regression was also applied for distance between paired points as an explanatory variable and the 95% confidence boundaries (both upper and lower) as response variables. Since we selected some burned sites far from their neighbouring unburned sites, we want to see whether these confidence intervals of RE values are increasing as a result of distance between them. Figure 3-2 shows some paired reference sites and the distance between each pair.

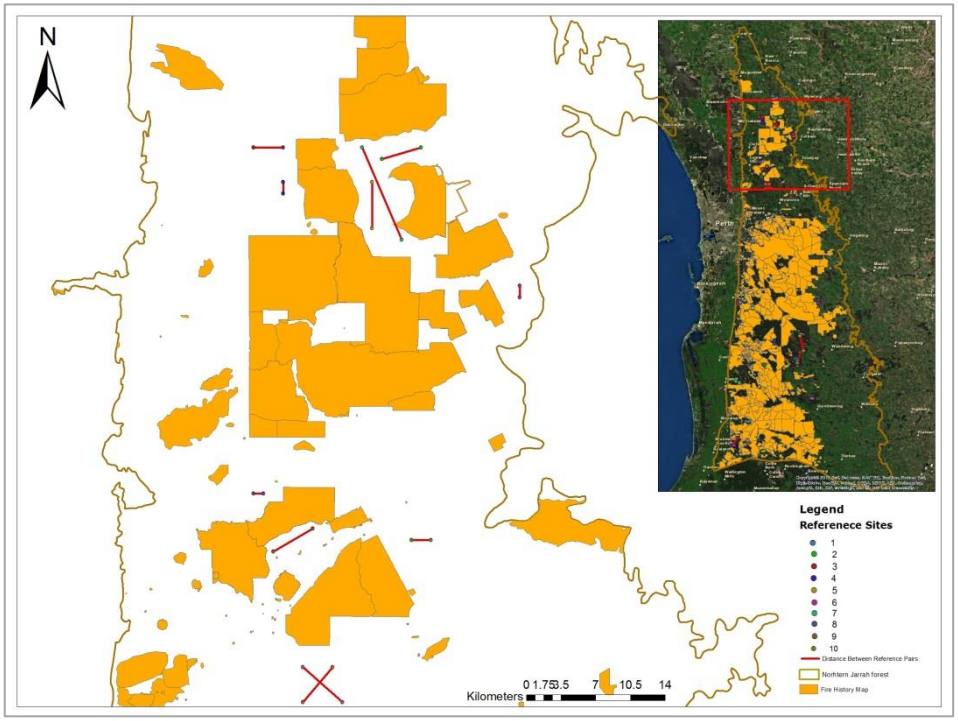

Figure 3-2. Unburned reference sites with different distances between each pair

3.5 RE variability in the absence of fire

To estimate possible effect of time and background noise on RE values in the absence of fire, regression with time as an explanatory variable and the 95% confidence boundaries (both upper and lower) of RE values was applied. We assume that RE values would not be consistent over time. Since for fire detection the threshold is set to the lower bound of the 95% confidence interval, we want to know whether this threshold is influenced by temporal fluctuations (since climate changes gradually).

3.6 Detection of fire signals

Wildfires may produce a clear drop in NDVI values (Diaz-Delgado et al., 2002). To assess if we can detect fire signals from NDVI time series (first research question); RE for each site (both burned and unburned sites) was computed. For this study, 30 unburned pairwise and 47 burned pairwise sites were selected. A reference dataset that compared 30 pairs of undisturbed sites with each other was created to see what the variability for this indicator is. The average of RE values of the 30 paired reference sites and their confidence interval of 95% and 99% were computed to obtain a lower threshold for this

indicator. In this case, it is hypothesized that when there is a sharp drop in the RE value of burned sites below this threshold, it indicates that a fire event took place.

3.7 Determination of the recovery p*eriod*

By the use of time series of satellite images, it is feasible to study and gain further insights in post-fire vegetation dynamics over large regions and long time periods (Diaz-Delgado et al., 2002). Several authors have used NDVI time series to analyse plant regeneration after fire (Diaz-Delgado et al., 2002 ; Viedma, et al., 1997). To estimate the recovery of vegetation (i.e., level of resilience) following detection of fires in section 3.6, forest state index (RE) was calculated. This was done by computing the ratio of the NDVI values for each date in the burned area over the NDVI value for the unburned neighbouring pixel (for each available NDVI in the time-series). RE of disturbed sites was compared with the RE of control (undisturbed) sites to estimate the recovery time to normal seasonal cycle (See Figure 3-3).

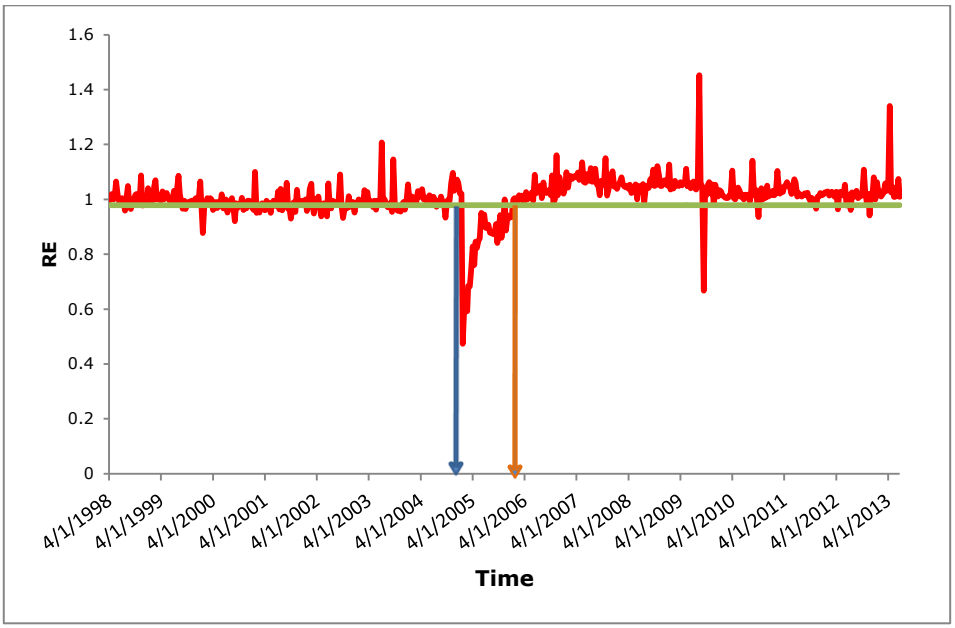

Figure 3-3. Recovery period of detected burned site (in red) through lower boundary of RE values of reference sites (in green). Blue arrow indicates date of fire occurrence and brown arrow shows its recovery date to normal cycle.

3.7.1 Sensitivity analysis

There were some drops in the data, detected as fires which were not real fires. The characteristic of a fire is that there is a drop followed by recovery period, but not all the drops were fires. So detected fires and their recovery period to normal seasonal cycle through the defined method, was required to check for its accuracy by sensitivity analysis. An IDL script written by Willem Nieuwenhuis was used which recorded moments in which RE values dropped below the lower confidence level of 95% and 99% of RE values of reference sites. To estimate the accuracy of this method, we increased the period that a signal should be below the threshold (i.e. an increasing time-window) to be identified as a fire, and compared the identified fire dates with the records from the fire history database. For every time-window size, the user's and producer's accuracy were computed. The user's accuracy refers to the probability that a detected fire corresponds to an actual fire on the ground while the producer's accuracy represents the probability that an actual fire is not detected. By these definitions, the time window size and confidence level which gives the highest user's accuracy was selected for further analysis.

3.8 Fire frequency and precipitation effect on recovery period

To assess the effect of climate factors on recovery period, first, monthly precipitation values of each pixel were assigned to the selected sites. Then, the unit of the pixel values was converted from m/day to mm/month in the corresponding dbf file. Annual precipitation and mean annual precipitation was computed for each selected burned site. A simple regression model with mean annual precipitation as an explanatory variable was applied to test the effect of precipitation on recovery period of burned sites. For more precise exploration, rainfall (mm) was calculated for three different periods:

(i) Growing season (i.e., winter, June-August) before the fire event
(ii) During the month of the fire. Since RE values are 10 daily (1st, 11th, 21th) and precipitation is a monthly dataset, to compute the rainfall in the fire month, a weighted equation for the fires which occurred on 11th or 21th, depending on the time of the fire event was applied.
(iii) After the fire, during the normal recovery period (2 years) for the correctly detected burned sites only (n =20)

Rainfall for growing season was selected based on the data observation of Figure 3-4 which was consistent with the data from Bates et al. (2008)(See Figure 2-2).

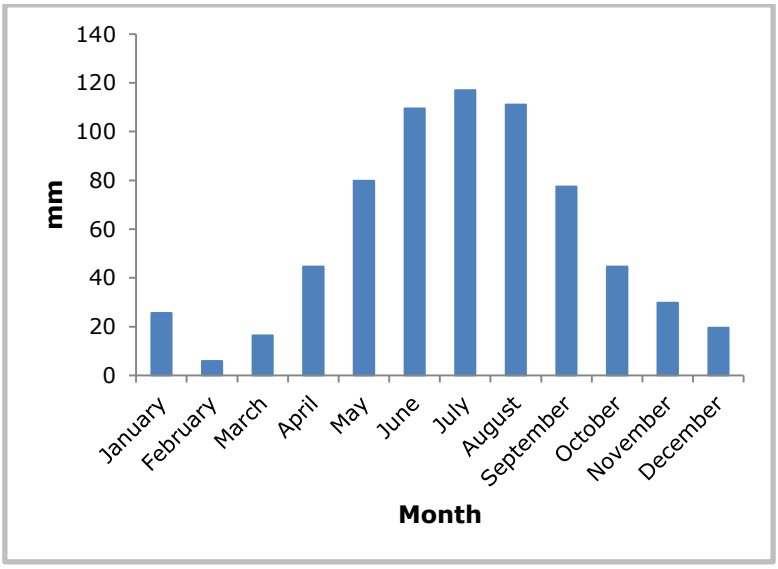

Figure 3-4. Average monthly rainfall (mm) for the selected sites of study area

Additionally, time since last fire up to current fire was computed for all correctly detected burned sites to assess the effect of fire frequency on recovery period.

3.8.1 Collinearity and regression analysis

Collinearity analysis was undertaken for the variables that were included in the regression analysis. Collinearity analysis was done by computing the Variance Inflation Factor (VIF) values for four explanatory variables mentioned in section 3.8. By the VIF values, the level of collinearity between the continuous explanatory variables was checked to see if the collinearity between variables reached the acceptable level. See equation (4) below:

$$VIF=1 / (1-R^2) \qquad \text{Equation (4)}$$

R^2 is the coefficient of determination calculated from linear regression of each explanatory variable against the response variable (recovery period). As R^2 approaches 1, VIF value results in an indefinite number. Therefore, VIF larger than 10 shows strong influence of collinearity. The VIF of the variable were computed using linear regression and in the last phase, stepwise regression analysis of Equation (5) was undertaken to omit the most unimportant predictors (explanatory variables). These predictors were: rainfall in growing season, rainfall during the month of fire, rainfall during the recovery period and time since last fire which mentioned in section 3.8 . All

statistical analyses for this section were undertaken using R (Version 3.0.1).

$Y = a + b*(P_1) + c*(P_2) + d*(P_3) + e*(P4)$ Equation (5)

Where a is the intercept and b, c, d and e are the slope coefficients of the model.

4. Results

4.1 Distance and time effect on of RE values

Figure 4-1 shows the RE values of 30 reference sites that were plotted against the distance between each pair. The regression line of distance between paired points as an explanatory variable and 99% confidence boundaries (both upper and lower) added to the plot, based on Table 4-1.

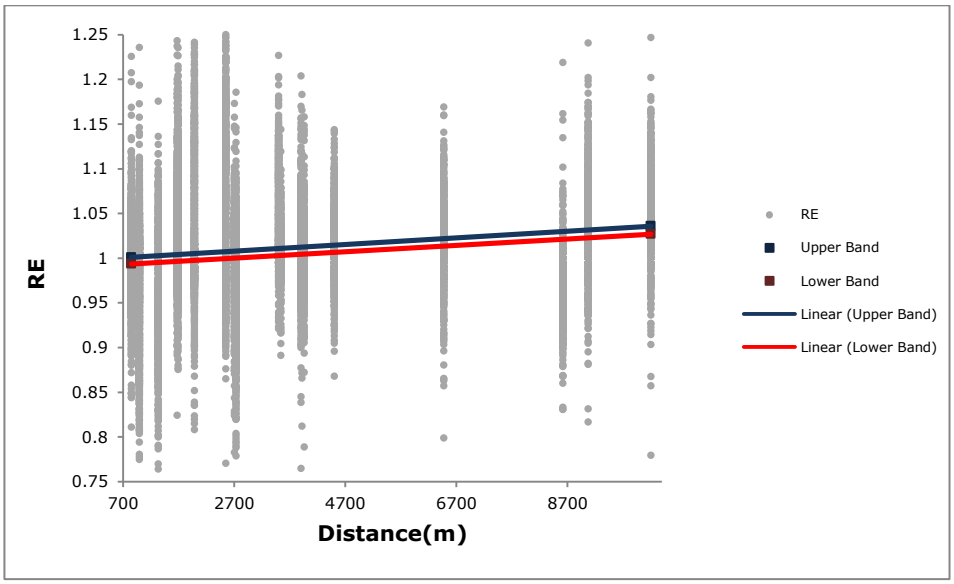

Figure 4-1. 99% Confidence interval of RE values over distance (m) of pairwise sites

Figure 4-1 illustrates that there is a positive non-significant slope in both upper and lower band of 99% of the confidence interval of RE values over distance. It means that there is a very slight slope in upper and lower band as a result of increased distance, indicating non-significant effect of distance on RE values.

Table 4-1. Regression of 99% confidence interval of RE values over distance (m)

		Coefficients	Standard Error	P-value
Upper band	Intercept	0.99	0.01	$8.5\ 10^{-39}$
	Distance	$3.73\ 10^{-06}$	$2.3\ 10^{-06}$	0.11
Lower Band	Intercept	0.99	0.01	$4.31\ 10^{-39}$
	Distance	$3.55\ 10^{-06}$	$2.23\ 10^{-06}$	0.12

Above mentioned table is the summary of the linear regression analysis which was applied for the 99% interval upper and lower band of RE values against distance. Results is robust to the specification of the dependant variable (the results are equivalent for both the upper band and the lower band of the RE values). The estimated slope is almost equal to zero, even when accounting for the units of the distance.

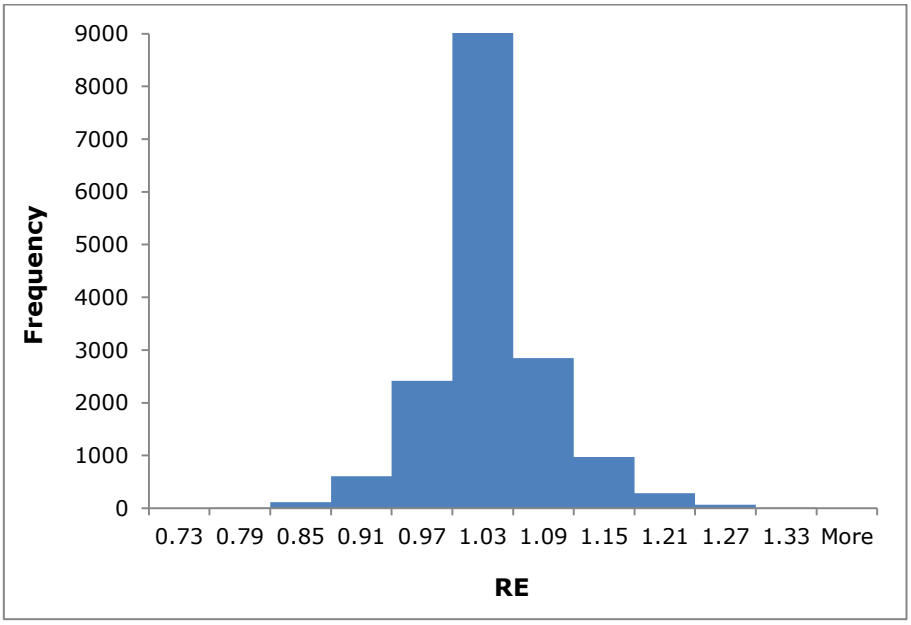

Figure 4-2. Histogram of RE values for reference sites

Figure 4-2 represents the distribution of RE values for reference sites. This histogram shows that RE values of reference sites are symmetrically distributed. Most of the values are between 0.97 and 1.09 which logically was expected for reference sites (since the reference sites are not disturbed so they should have similar NDVI values).

For more examinations, regression analysis of pairwise distance as an explanatory variable and the first quartile, median and third quartile as the response variables was undertaken. The summary of these regressions is presented in Table 4-2.

Table 4-2. Regression of First quartile, second quartile and Median of RE against distance

		Coefficients	Standard Error	P-value
First quartile	Intercept	0.97	0.01	$2.45\ 10^{-38}$
	Distance	$3.3\ 10^{-06}$	$2.31\ 10^{-06}$	0.16
Median	Intercept	0.99	0.99	$1.25\ 10^{-38}$
	Distance	$3.55\ 10^{-06}$	$3.558\ 10^{-06}$	0.14
Second quartile	Intercept	1.02	0.01	$7.42\ 10^{-36}$
	Distance	$4.02\ 10^{-06}$	$3\ 10^{-06}$	0.19

These models did not show any significant effect of distance on the variability or mean value of RE (Table 4-2). Therefore, the distances between burned sites and their control sites that were used in our dataset were assumed to have non-significant effect on the signal or the quality of the data that was used in the subsequent steps.

Similar to Figure 4-1, RE values of the unburned 30 reference sites was plotted over time. Figure 4-3 represents the regression of 99% of the confidence interval (both upper and lower) of RE values against time (through Table 4-3).

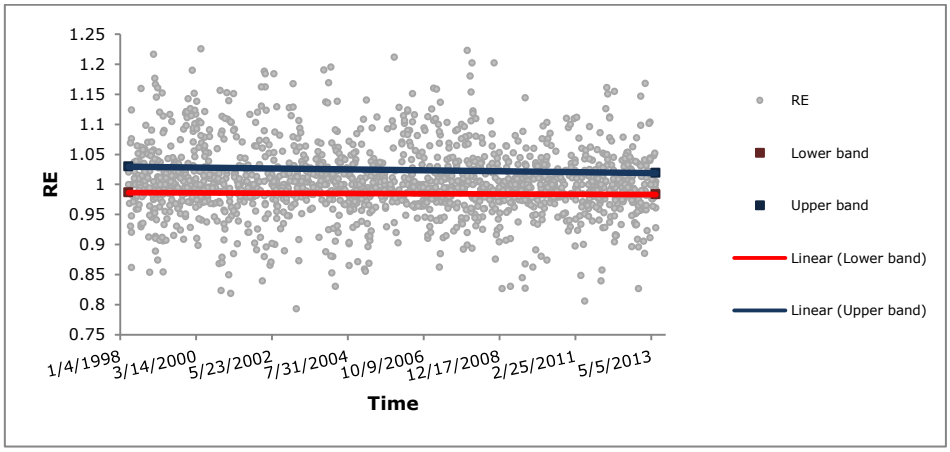

Figure 4-3. 99% Confidence interval of RE values over time

Table 4-3. Regression of 99% confidence interval of RE values over time

		Coefficients	*Standard Error*	*P-value*
Upper band	Intercept	1.09	0.01	0
	Time	$-1.9\ 10^{-06}$	$3.19\ 10^{-07}$	$3.09\ 10^{-09}$
Lower Band	Intercept	1.0	0.08	0
	Time	$5.43\ 10^{-07}$	$2.07\ 10^{-07}$	0.01

Based on the finding through regression analysis (Table 4-3), RE values of reference sites are varying around one over time. According to the 99% confidence interval, we can claim that there is not a significant effect on RE values as a result of time (the estimated slopes in Table 4-3 are strongly significant and almost equivalent to zero).

4.2 Sensitivity analysis

Table 4-4 displays the user's and producer's accuracy of the fire detection approach using either a 95% or 99% confidence interval of reference values and then applying different time window sizes.

Table 4-4. Sensitivity analysis for detected fires through increased time window size within 95% and 99% confidence interval of reference RE values

95% confidence interval			99% confidence interval		
Window Size(day)	User's accuracy	Producer's accuracy	Window Size(day)	User's accuracy	Producer's accuracy
60	0.15	0.78	60	0.18	0.76
120	0.23	0.66	120	0.26	0.60
180	0.32	0.54	180	0.35	0.49
240	0.35	0.45	240	0.40	0.43
300	0.36	0.36	300	0.39	0.32
360	0.38	0.28	360	0.41	0.26
420	0.40	0.25	420	0.37	0.21
480	0.39	0.22	480	0.38	0.18
540	0.36	0.18	540	0.37	0.16
600	0.13	0.34	600	0.38	0.15
660	0.10	0.32	660	0.35	0.11
720	0.27	0.07	720	0.33	0.09

Above mentioned table reveals that by the 99% confidence interval and the 360 days as an optimal time window size, we can get highest correctly detected fires with, user's accuracy of 0.41 (a bit higher than the 95% confidence interval and 420 days of time window size, which have a user's accuracy of 0.40).

4.3 Fire signal detection

Corresponding to the first research objective, fire signals were detected by the use of lower confidence interval of RE values of reference sites. Of a total of 47 burned sites, 20 fires were correctly detected. Figure 4-4 illustrates the location of the detected fire signals based on fire history map. Figure 4-5 and Figure 4-6 are two examples of these detections with the illustration of occurrence date and detected fire signal. This method responds better for big fires with substantial deviation from the threshold than small fires.

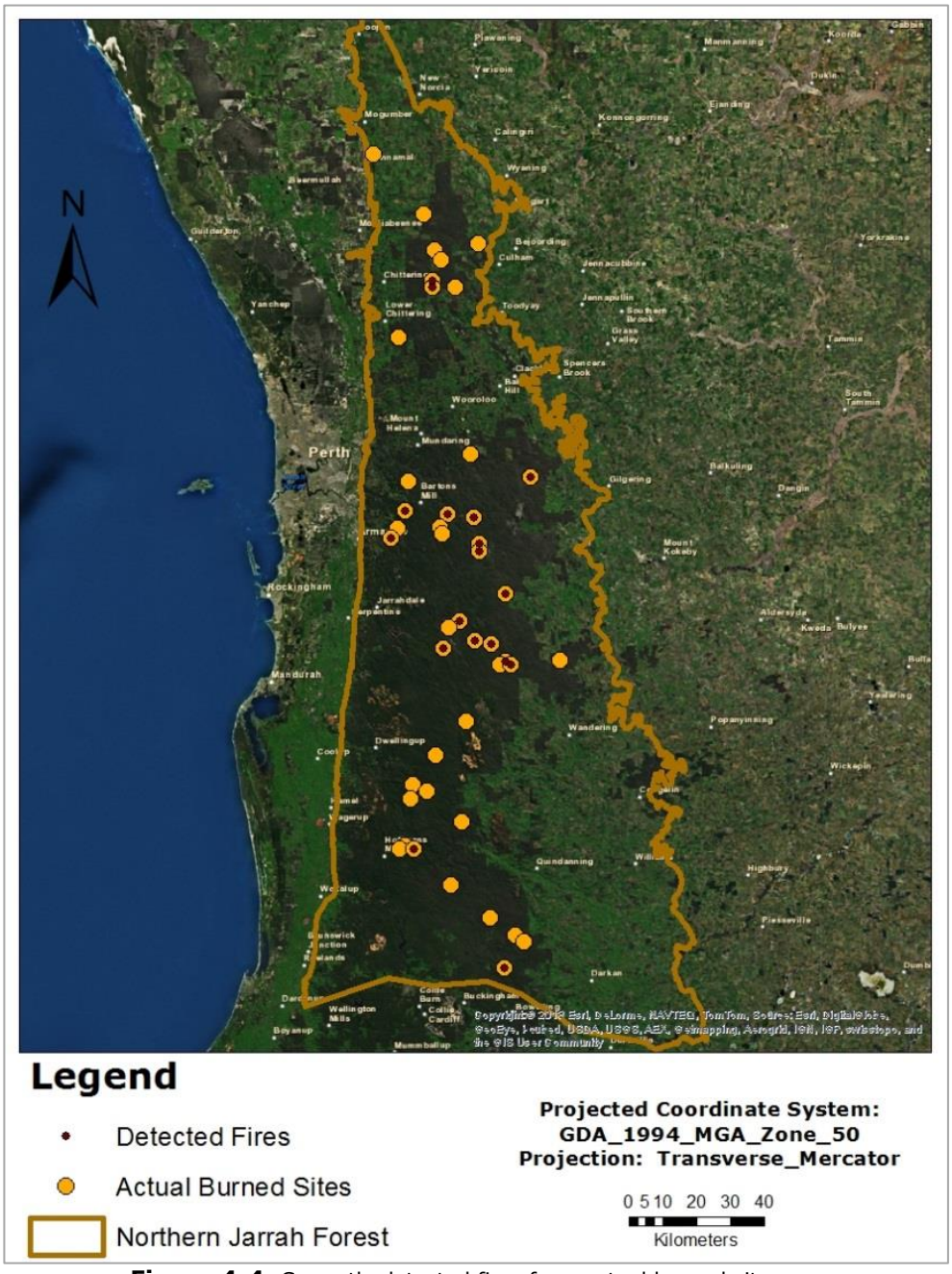

Figure 4-4. Correctly detected fires from actual burned sites

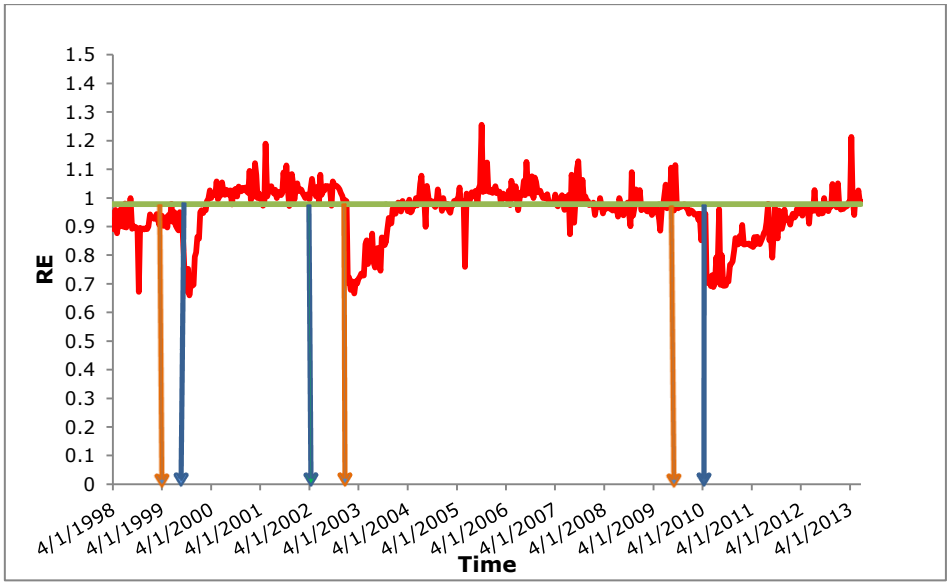

Figure 4-5. Detected fires by comparing their RE values (red) with lower confidence interval of reference values (green). Blue arrows indicate the date of the fire in the fire history map and brown arrows show estimated fire date.

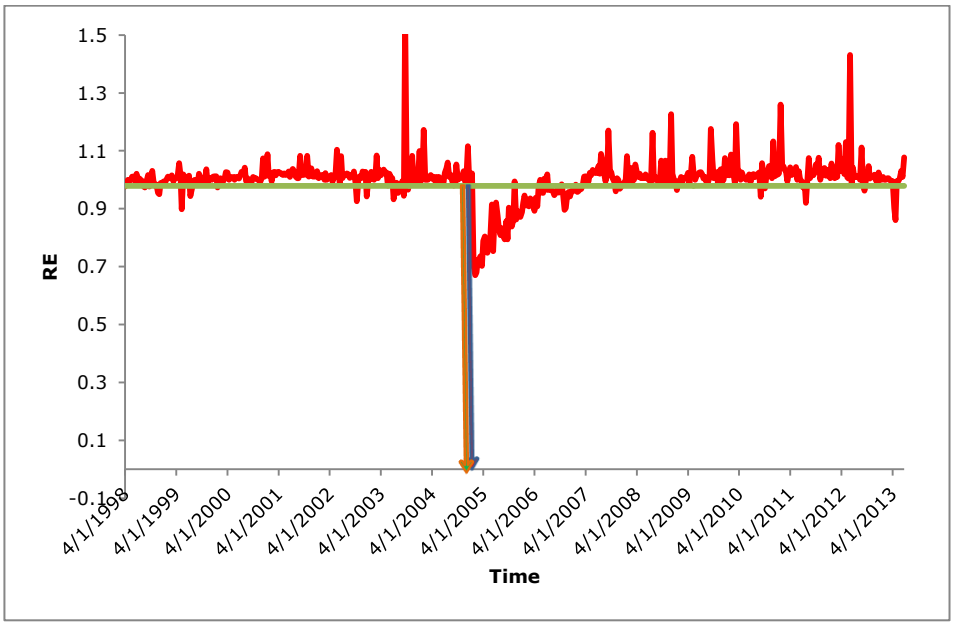

Figure 4-6. Detected fires by comparing their RE values (red) with lower confidence interval of reference values (green). Blue arrow indicates the date of the fire in the fire history map and brown arrow shows estimated fire date.

Figure 4-5 and Figure 4-6 illustrate detected fires which compares their occurrence dates with the date of occurrence indicated in the fire history map.

4.4 Fire recovery period to normal cycle

The script used for fire detection was applied to detect the fire recovery period with 95% and 99% confidence interval. Table 4-5 shows the result for correctly detected fires with 99% of confidence interval as an optimal confidence level. The recovery period of 20 correctly detected fires to the normal cycle of unburned sites is showed in Table 4-5. In this table the start date indicates the time of occurrence and end date indicates the time to back to normal cycle.

Table 4-5. Correctly detected fire signals and their recovery period to normal cycle

Start date	End date	Recovery period(days)
11/7/2009	11/6/2010	335
21/12/2002	1/12/2003	345
21/1/2005	1/1/2006	345
11/1/2003	11/1/2004	365
1/12/2004	11/12/2005	375
1/2/2007	11/2/2008	375
11/4/1998	1/6/1999	416
11/1/2005	1/4/2006	445
21/11/2002	21/2/2004	457
11/12/2002	21/4/2004	497
11/10/2002	11/5/2004	578
11/10/2004	1/7/2006	628
1/4/1998	21/2/2000	691
21/2/2000	21/11/2001	639
21/5/2006	1/6/2008	742
21/1/2005	1/3/2007	769
21/12/2001	1/5/2004	862
11/11/2006	1/4/2009	872
11/8/2000	11/1/2004	1248
11/7/2009	11/3/2013	1339

Figure 4-7 presents the above mentioned fires location with their recovery period to the normal cycle.

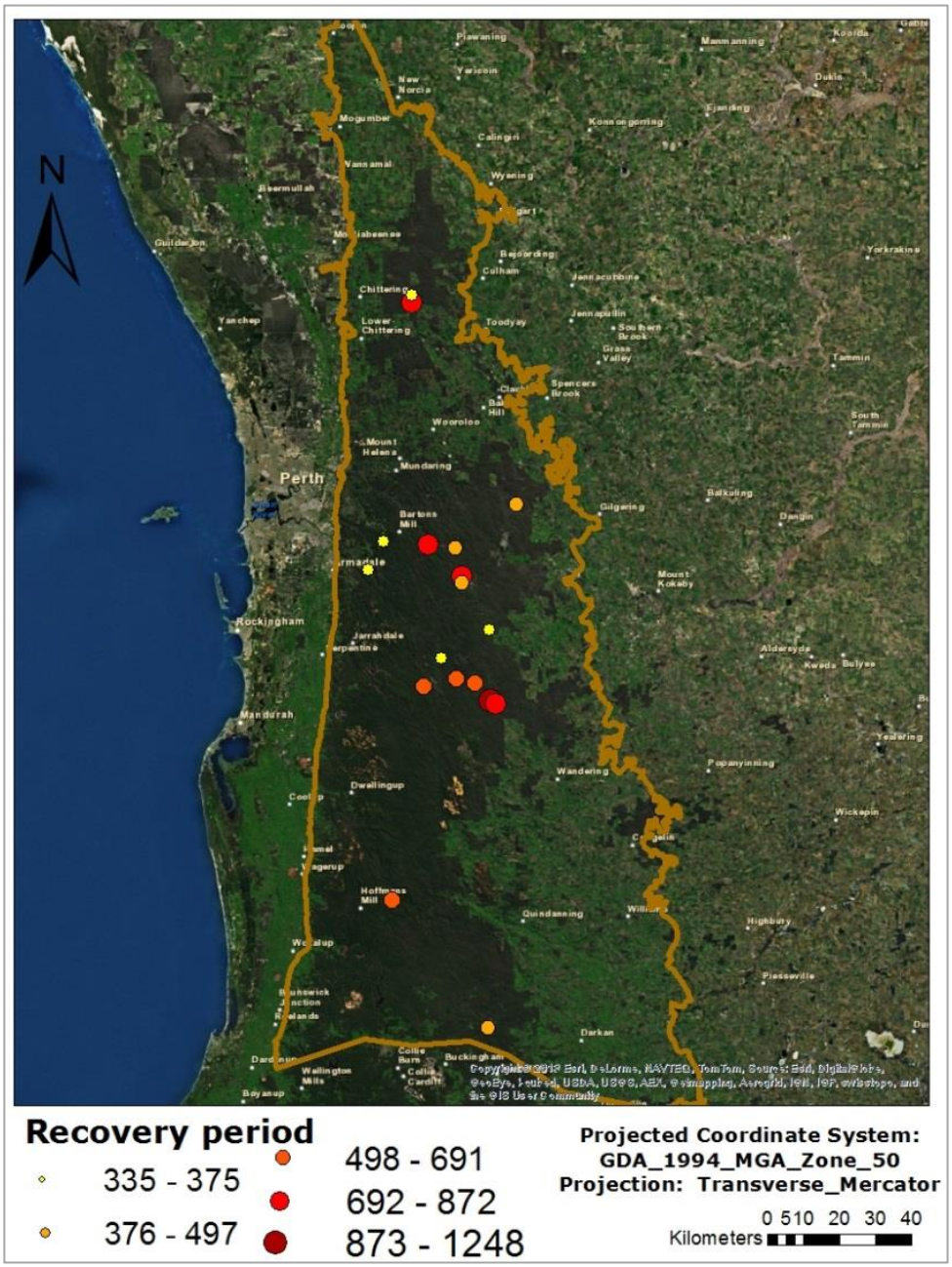

Figure 4-7. Map of detected fire signals and their recovery period to normal cycle

4.5 Collinearity analysis

Collinearity analysis was performed by VIF computation for 20 correctly detected fire signals. The results of VIF calculation have been represented in Table 4-6.

Table 4-6. VIF values for collinearity analysis

Variable	VIF
P_1	1.219
P_2	1.161
P_3	1.151
P_4	1.036

P_1 = precipitation during the growing season
P_2 = precipitation in the fire month
P_3 = precipitation during the recovery period
P_4 = Time since last fire (fire frequency)

According to Table 4-6, VIF values were all less than two. This indicates that there is no serious collinearity between the four explanatory variables, which can adversely affect the regression analysis.

4.6 Rainfall and fire frequency effects on recovery time

Stepwise regression was performed to estimate the best fit model. The model was developed through multiple regressions. In the stepwise regression, the fire frequency variable was omitted from the model. This means that, apparently, the frequency of fire does not have a significant effect on recovery period of burned sites and it does not contribute to explain the overall variation of the recovery period (the goodness of fit for the full model is worse than the reduced version model reported in the Table 4-7). Table 4-7 and Table 4-8 shows the summary of the best fit model with only three variables.

Table 4-7. Summary of multiple regressions for prediction of recovery period

	Estimate	Std. Error	t value	Pr(>|t|)
Intercept	300.2170	171.6229	1.749	0.099395
P_1	-0.819	0.4164	-1.968	0.066616
P_2	2.9097	0.9128	3.188	0.005724
P_3	0.4961	0.1002	4.950	0.000145

Table 4-8. Summary of goodness of fit

Test statistic/Parameters	Value
R_2	0.6953
Adjusted R_2	0.6382
F_statistics	12.17
P_value	0.0002118

Though R_2 value is not great but the model is quite good in the sense that all coefficients are significant (at a 90% significance level) despite the relatively small number of data points. Further, the F-statistic strongly supports that the model is correctly specified (significance over 99%).

According to the stepwise regression, rainfall during the wet season shows a non-significant and negative relationship with recovery period (or time). Rainfall during the fire event and during the recovery period showed a significant positive relationship with recovery period which contradicts the hypothesis (Table 4-7).This means that with high amount of precipitation during the growing season, the recovery period decreases, while with high amount of precipitation during the fire event, recovery time grows longer. Precipitation during the recovery period has the same effect on recovery time as precipitation during the fire month does.

5. Discussion

This research investigated whether SPOT NDVI time series could detect fire signals. Moreover NDVI was used to estimate post-fire recovery period by the use of forest state index (RE). Because NDVI is sensitive to seasonal variation of green biomass (Huete et al., 2002), the RE was used, as it minimizes the effect of seasonal and inter-annual variation in phenology (Diaz-Delgado et al., 2002). Only less than half of selected burned sites from the fire history map could be detected. This could be due to uncertainty in the data model (the fire history map).

Probably, only big fires which had substantial drop in RE values were detected. Most of these detected fires occurred in the dry season (i.e., summer, December-February). To evaluate the size and intensity of the detected fires, it would be possible to examine burned areas on Landsat-type imagery. The limitations in detecting fires seem to be related to the smaller wet season fires which in turn might be related with the opposite signs that were found between rainfall and recovery period than anticipated.

Despite the compositing technique used by the data provider to construct the 10-daily SPOT NDVI dataset, which reduces atmospheric effects, persistent cloud cover or otherwise moist atmospheric conditions may cause poor (i.e. low) NDVI values in the dataset that do not well relate to the vegetation condition on the ground (Pettorelli et al., 2005). A possible solution is the temporal filtering of the NDVI dataset. Moreover, these noises (false high and low NDVI values) which breaks the hypothesis of some standard statistical methods, cause more complexity when errors vary in time and space (Pettorelli et al., 2005). In this study, the data was not smoothed to maintain short-term variation in NDVI which can in fact represent changes in vegetation. Nonetheless, given the larger recovery times (of several 10-day periods) filtering would most likely not have a negative effect on fire detection potential, and by reducing noise, even improve it.

It is remarkable that different species including *Eucalyptus marginata* in SWA are not sensitive to fire, although their response is different within and between species (Wardell-Johnson, 2000). The regeneration of *Eucalyptus marginata* is well adapted to variable and seasonal climate. These species can grow rapidly in response to favourable periods (Wardell-Johnson, 2000).

Following Wardell-Johnson (2000), the result of this research did not show any significant effect of fire frequency on the recovery period by

the regression analysis which was done against time since last fire (as fire frequency). However, Diaz-Delgado et al. (2002) found in Catalonia (north-eastern Spain) that NDVI derived recovery slows down after the second of two successive fires with less than 11 years separation. Their studies showed vegetation regeneration after 70 months was slower after the second fire than after the first fire. Not finding an effect of fire frequency on recovery in this study indicates, either the NJF system works differently from how we expected it to work or fire intensity might be much more important than fire frequency for explaining recovery times. In other words, sites with high intensity fires and lower fire frequency might be affected more than areas with low intense fires and high fire frequency. Information on fire intensity was not available in the fire history dataset. However, fire intensity perhaps could be a better explanatory variable for post-fire recovery time.

The results of this study indicate a weak negative correlation between recovery period and precipitation during the growing season. It was expected to find a stronger negative correlation but the absence of a strong correlation could be partially due to ignoring the intensity of rainfall which might be more important than total amount of rainfall. Perhaps forests do become more resilient when there is plenty of rain during the growing season, while the effect on the total fuel load (and through that the intensity of the fire, what we initially thought might be the logic) is negligible.

Also, a positive correlation between recovery and precipitation during the fire occurrence was found. As mentioned in the Introduction, high amounts of rainfall during the fire event were expected to cause highly wet vegetation and less intense fires, which should take shorter for forest to recover. But the results contradict this hypothesis. I suspect that, similarly to the previous one, light rain or drizzle will not have a strong effect on the vegetation during the fire event and, consequently, on their recovery period.

Lastly, a positive (significant) correlation between precipitation during the recovery period and the recovery period itself was found. We assume that high amounts of rainfall affect both reference sites and burned sites. The assumption is that the response of the vegetation to rainfall in burned and unburned sites is similar, while the response in an unburned site might be much faster/stronger than in an burned site

In addition, coarse resolution (1x1 km) of the pixels in this research itself has some potential limitation. If an entire pixel is affected by an

intense fire, it is more likely to be picked up. But some of the fires were not that large. Then, it is suggested that a higher-resolution NDVI series, such as MODIS could be used instead.

It is notable that simply SPOT NDVI was applied to estimate recovery periods. Although, the recovery period which was extracted from RE times series, we did not verify whether these "recovery periods" were matching recovery as observed on the ground. In order to evaluate if NDVI could estimate recovery times, ground reference data on recovery times would be needed to compare these estimates.

6. Conclusions and recommendations

6.1 Conclusions

Fire signals and their recovery to normal cycle were detected by comparison between RE values of burned sites and reference sites. Forest recovery period and its relation with fire frequency and amount of precipitation was examined to see if critical slowing down occurs in this ecosystem as a result of drought and fire frequency. Based on the obtained results, it is concluded that:

- Critical slowing down may not be happening in this system based on the achieved results and adaptability of the system to fire.

- Fire frequency does not seem to be a significant factor, which limits the model ability to explore critical slowing down. There is no clear indication that the phenomenon is occurring but this might be also due to the discussed limitations of the data.

6.2 Recommendations

The analysis of fire detection showed mixed results; some fires (big fires occurring in the summer period) were adequately identified but others were not. A critical assessment and improvement of both the detection method (in terms of the rules used but also of the input data) and the calibration data (the independent fire map used to verify if the model accurately predicted the fires) may contribute to improve the results of this research.

In order to investigate the forest recovery period and possible explanatory variables, it is important to consider the most influencing factors on the recovery period. It is recommended that more variables such as fire intensity and rainfall intensity, be included to explain the length of the recovery period after fire by investigation NDVI dataset.

This work did not consider the fire intensity as a major fire regime parameter, nor its influence on plant regeneration. Perhaps an alternative hypothesis of intensity affecting recovery time could be tested, which requires further research. By introducing some ancillary information like fuel accumulation or wind speed, the intensity level of each fire may be approximated. A better understanding of this issue may aid to estimate forest recovery period of burned areas under different fire intensity levels. Hence, to gain a better understanding of the ecosystem response to fire, it is recommended to incorporate levels of fire intensity into the analysis.

Additionally, ground reference data on recovery time of burned areas in study area can be collected for estimated recovery period evaluation.

Future research need to link the improved results using more complex statistical models to variables that explain the critical slowing down in the study area. However, this is only possible with bigger data samples and generally improved input data.

References

ALLEN, C. D., MACALADY, A. K., CHENCHOUNI, H., BACHELET, D., MCDOWELL, N., VENNETIER, M., KITZBERGER, T., RIGLING, A., BRESHEARS, D. D., HOGG, E. H., GONZALEZ, P., FENSHAM, R., ZHANG, Z., CASTRO, J., DEMIDOVA, N., LIM, J.-H., ALLARD, G., RUNNING, S. W., SEMERCI, A. & COBB, N. 2010. A global overview of drought and heat-induced tree mortality reveals emerging climate change risks for forests. *Forest Ecology and Management,* 259**,** 660-684.

ANDERSON, G. L., HANSON, J. D. & HAAS, R. H. 1993. Evaluating Landsat Thematic Mapper Derived Vegetation Indices for Estimating Above-Ground Biomass on Semiarid Rangelands. *REMOTE SENSING OF ENVIRONMENT -NEW YORK-,* 45**,** 165.

BATES, B., HOPE, P., RYAN, B., SMITH, I. & CHARLES, S. 2008. Key findings from the Indian Ocean Climate Initiative and their impact on policy development in Australia. *Climatic Change,* 89**,** 339-354.

BATES, B. C., KUNDZEWICZ, Z.W., WU, S., PALUTIKOF, J.P. . 2008. *Climate change and water* [Online]. IPCC Technical Paper IV. IPCC Secretariat, Geneva. Available: http://www.ipcc.ch/publications_and_data/publications_and_data_technical_papers.shtml.

BEERLING, D. J. 1993. Holocene book reviews: Climate change 1992. The supplementary report to the IPCC scientific assessment Edited by Houghton, J.T., Callander, B.A. and Varney, S.K. Cambridge : Cambridge University Press, 1992, 200 pp., £9.95, paperback. ISBN. *Holocene,* 3**,** 279.

BOND, W. J. & KEELEY, J. E. 2005. Fire as a global 'herbivore': the ecology and evolution of flammable ecosystems. *Trends in Ecology & Evolution,* 20**,** 387-394.

CARPENTER, S. R., LUDWIG, D. & BROCK, W. A. 1999. Management of eutrophication for lakes subject to potentially irreversible change. *Ecological Applications,* 9**,** 751-771.

CSIRO AND BOM 2007. Climate change in Australia - Technical Report. Australia: CSIRO.

DAKOS, V., CARPENTER, S. R., BROCK, W. A., ELLISON, A. M., GUTTAL, V., IVES, A. R., KEFI, S., LIVINA, V., SEEKELL, D. A., VAN NES, E. H. & SCHEFFER, M. 2012. Methods for Detecting Early Warnings of Critical Transitions in Time Series Illustrated Using Simulated Ecological Data. *Plos One,* 7.

DAKOS, V., SCHEFFER, M., VAN NES, E. H., BROVKIN, V., PETOUKHOV, V. & HELD, H. 2008. Slowing down as an early warning signal for abrupt climate change. *Proceedings of the National Academy of Sciences of the United States of America,* 105**,** 14308-14312.

DAKOS, V., VAN NES, E. H., DONANGELO, R., FORT, H. & SCHEFFER, M. 2010. Spatial correlation as leading indicator of catastrophic shifts. *Theoretical Ecology,* 3**,** 163-174.

DELL, B. & HAVEL, J. J. 1989. The jarrah forest, an introduction. *In:* DELL, B., HAVEL, J. J. & MALAJCZUK, N. (eds.) *The Jarrah Forest.* Springer Netherlands.

DIAZ-DELGADO, R., LLORET, F., PONS, X. & TERRADAS, J. 2002. Satellite evidence of decreasing resilience in Mediterranean plant communities after recurrent wildfires. *ECOLOGY -NEW YORK-,* 83**,** 2293-2303.

FAO. 2006. *Global forest resources assessment* [Online]. Rome: Food and Agriculture Organization of the United Nations. Available: http://www.fao.org/countryprofiles/index/en/?iso3=AUS&paia=5 [Accessed 1-Augest 2013].

FOLKE, C., CARPENTER, S., WALKER, B., SCHEFFER, M., ELMQVIST, T., GUNDERSON, L. & HOLLING, C. S. 2004. Regime Shifts, Resilience, and Biodiversity in Ecosystem Management. *Annual Review of Ecology, Evolution, and Systematics,* 35**,** 557-581.

GAMON, J. A., FIELD, C. B., GOULDEN, M. L., GRIFFIN, K. L., HARTLEY, A. E., JOEL, G., PEÑUELAS, J. & VALENTINI, R. 1995. Relationships Between NDVI, Canopy Structure, and Photosynthesis in Three Californian Vegetation Types. *Ecological Applications,* 5**,** 28-41.

GENTILLI, J. 1989. The jarrah forest, Climate of the Jarrah forest. *In:* DELL, B., HAVEL, J. J. & MALAJCZUK, N. (eds.) *The Jarrah Forest, a complex Mediterranean ecosystem.* Springer Netherlands.

GILL, A. M. 1975. Fire and The Australian Flora: A Review. *Australian Forestry,* 38**,** 4-25.

GOLDAMMER, J. G. 1990. Fires and their effects in the wet-dry tropics of Australia. *Fire in the tropical biota.* University of Freiburg, Bertoldstrabe 17, 7800 Freiburg, FRG: Institute of Forest Zoology.

GOVERNMENT OF WESTERN AUSTRALIA. 2013. *Fuel loads and fire intensity* [Online]. Available: http://www.dpaw.wa.gov.au/management/fire/fire-and-the-environment/51-fuel-loads-and-fire-intensity [Accessed 6-February 2014].

GRANZOW-DE LA CERDA, Í., LLORET, F., RUIZ, J. E. & VANDERMEER, J. H. 2012. Tree mortality following ENSO-associated fires and drought in lowland rain forests of Eastern Nicaragua. *Forest Ecology and Management,* 265**,** 248-257.

HEDDLE, E. M., HAVEL, J. J. & LONERAGAN, O. W. 1980. Vegetation Complexes of the Darling System, Western Australia. *Atlas of*

Natural Resources Darling System, Western Australia. Department of Conservation and Environment, Perth.

HOPPER, S. D. & GIOIA, P. 2004. The Southwest Australian Florisitic Region: evolution and conservation of a global hotspot of biodiversity. *Annual Review of Ecology, Evolution and Systematics,* 35**,** 623-650.

HUETE, A., DIDAN, K., MIURA, T., RODRIGUEZ, E. P., GAO, X. & FERREIRA, L. G. 2002. Overview of the radiometric and biophysical performance of the MODIS vegetation indices. *Remote Sensing of Environment,* 83**,** 195-213.

IPCC 2007. Climate Change 2007: The Physical Science Basis. Contribution of Working Group I to the Fourth Assessment Report of the Intergovernmental Panel on Climate Change. *In:* SOLOMON, S., QIN, D., MANNING, M., CHEN, Z., MARQUIS, M., AVERYT, K. B., TIGNOR, M. & MILLER, H. L. (eds.). Cambridge University Press, Cambridge, United Kingdom and New York, NY, USA.

KLAUSMEYER, K. R. & SHAW, M. R. 2009. Climate Change, Habitat Loss, Protected Areas and the Climate Adaptation Potential of Species in Mediterranean Ecosystems Worldwide. *PLoS ONE,* 4**,** e6392.

LAURANCE, W. F., DELL, B., TURTON, S. M., LAWES, M. J., HUTLEY, L. B., MCCALLUM, H., DALE, P., BIRD, M., HARDY, G., PRIDEAUX, G., GAWNE, B., MCMAHON, C. R., YU, R., HERO, J.-M., SCHWARZKOPF, L., KROCKENBERGER, A., DOUGLAS, M., SILVESTER, E., MAHONY, M., VELLA, K., SAIKIA, U., WAHREN, C.-H., XU, Z., SMITH, B. & COCKLIN, C. 2011. The 10 Australian ecosystems most vulnerable to tipping points. *Biological Conservation***,** Published online: 21 February 2011.

LOTSCH, A., FRIEDL, M. A., ANDERSON, B. T. & TUCKER, C. J. 2003. Coupled vegetation-precipitation variability observed from satellite and climate records. *Geophysical Research Letters,* 30**,** CLM 8-1 - 8-4.

LUDWIG, D., WALKER, B. & HOLLING, C. S. 1997. *Sustainability, stability, and resilience / Donald Ludwig, Brian Walker, Crawford S. Holling*, Stockholm, 1997.

MATUSICK, G., RUTHROF, K., BROUWERS, N., DELL, B. & HARDY, G. J. 2013. Sudden forest canopy collapse corresponding with extreme drought and heat in a mediterranean-type eucalypt forest in southwestern Australia. *European Journal of Forest Research,* 132**,** 497-510.

MYERS, N., MITTERMEIER, R. A., MITTERMEIER, C. G., DA FONSECA, G. A. B. & KENT, J. 2000. Biodiversity hotspots for conservation priorities. *Nature,* 403**,** 853-858.

PEEL, M. C., FINLAYSON, B. L. & MCMAHON, T. A. 2007. Updated world map of the Koppen-Geiger climate classification. *Hydrology and Earth System Sciences,* 11**,** 1633-1644.

PETTORELLI, N., VIK, J. O., MYSTERUD, A., GAILLARD, J.-M., TUCKER, C. J. & STENSETH, N. C. 2005. Using the satellite-derived NDVI to assess ecological responses to environmental change. *Trends in Ecology & Evolution,* 20**,** 503-510.

SCHEFFER, M., BASCOMPTE, J., BROCK, W. A., BROVKIN, V., CARPENTER, S. R., DAKOS, V., HELD, H., VAN NES, E. H., RIETKERK, M. & SUGIHARA, G. 2009. Early-warning signals for critical transitions. *Nature,* 461**,** 53-59.

SCHEFFER, M., CARPENTER, S., FOLEY, J. A., FOLKE, C. & WALKER, B. 2001. Catastrophic shifts in ecosystems. *Nature,* 413**,** 591-596.

SCHEFFER, M., HOSPER, S. H., MEIJER, M. L., MOSS, B. & JEPPESEN, E. 1993. Alternative equilibria in shallow lakes. *Trends in Ecology & Evolution,* 8**,** 275-279.

TARNAVSKY, E., GARRIGUES, S. & BROWN, M. E. 2008. Multiscale geostatistical analysis of AVHRR, SPOT-VGT, and MODIS global NDVI products. *Remote Sensing of Environment,* 112**,** 535-549.

TILMAN, D., FARGIONE, J., WOLFF, B., D'ANTONIO, C., DOBSON, A., HOWARTH, R., SCHINDLER, D., SCHLESINGER, W. H., SIMBERLOFF, D. & SWACKHAMER, D. 2001. Forecasting Agriculturally Driven Global Environmental Change. *Science,* 292**,** 281-284.

UOC. 2003. *Global warming* [Online]. Union Of Concerned Scientists. Available: http://www.ucsusa.org/global_warming/science_and_impacts/impacts/early-warning-signs-of-global-4.html [Accessed 23-January 2014].

VAN NES, E. H. & SCHEFFER, M. 2007. Slow recovery from perturbations as a generic indicator of a nearby catastrophic shift. *American Naturalist,* 169**,** 738-747.

VIEDMA, O., MELIÁ, J., SEGARRA, D. & GARCIA-HARO, J. 1997. Modeling rates of ecosystem recovery after fires by using landsat TM data. *Remote Sensing of Environment,* 61**,** 383-398.

WARDELL-JOHNSON, G. W. 2000. Responses of forest eucalypts to moderate and high intensity fire in the Tingle Mosaic, south-western Australia: comparisons between locally endemic and regionally distributed species. *Austral Ecology,* 25**,** 409-421.

WISSEL, C. 1984. A universal law of the characteristic return time near thresholds. *Oecologia,* 65**,** 101-107.

WITTENBERG, L., MALKINSON, D., BEERI, O., HALUTZY, A. & TESLER, N. 2007. Spatial and temporal patterns of vegetation recovery following sequences of forest fires in a Mediterranean landscape, Mt. Carmel Israel. *CATENA,* 71**,** 76-83.